IARJSET ISSN (O) 2393-8021, ISSN (P) 2394-1588

International Advanced Research Journal in Science, Engineering and Technology

Impact Factor 8.066 ⁜ Peer-reviewed & Refereed journal ⁜ Vol. 13, Issue 6, June 2026

DOI: 10.17148/IARJSET.2026.13654

Numerical Investigation of Blood Rheology and Phase Distribution in Micro-Arterial Networks

Vishanu Mohan Sharma[1*], Dr. Dileep Singh[2]

Research Scholar, Department of Mathematics, J.S. University, Shikohabad (India)[1]

Assistant Professor, Department of Mathematics, J.S. University, Shikohabad (India)[2]

*Corresponding Author

Abstract: Blood flow in micro-arterial networks exhibits complex non-Newtonian behavior due to the rheological properties of blood and the unequal distribution of red blood cells at vascular bifurcations. This study numerically investigates blood rheology and phase distribution using a Bingham plastic model combined with hematocrit-dependent viscosity and plasma-skimming effects. In this study, the equations describing the flow of blood through the network of blood vessels have been solved in order to determine how mass, momentum, and hematocrit (the ratio of red blood cells to total blood) will distribute during steady state laminar flow. Both analytical and numerical results show that a central "plug-flow" region is developed; that there are non-linear relationships between the velocity of blood flow and shear rates at various locations within the vessel; and that the amount of hematocrit present in each of the two daughter vessels differs significantly from one another. The larger daughter vessel has a high concentration of red blood cells relative to its size, which increases its overall viscosity as well as it's ability to resist flow. Conversely, the smaller daughter vessel contains a low concentration of red blood cells and therefore has a lower viscosity than the larger vessel. Overall, the model accurately describes plasma skimming and illustrates a direct relationship between hematocrit levels and the rheological properties of blood throughout the microvascular system thereby illustrating potential implications for tissue perfusion.

Keywords: Micro-arterial networks, Bingham plastic fluid, Blood rheology, Hematocrit transport, Plasma skimming, Phase separation, Non-Newtonian blood flow, Microcirculation

I. INTRODUCTION

The microcirculation is important for delivering oxygen, nutrients and removing waste from the body's tissues. In addition to factors such as vessel dimensions and red blood cell spatial distribution, the non-Newtonian viscoelastic behavior of blood at low-shear rates affects the fluid dynamics in micro-arterial networks. Specifically, the non-linear relationship between shear stress and strain rate that characterizes the behavior of blood results in both yield stress and dependence on hematocrit concentration. Furthermore, when red blood cells encounter each other at very low flow velocities, they may interact with one another rather than flowing freely through the vessel. These same effects cause an uneven division of red blood cells at branching points in microvascular networks (plasma skimming) which can create significant variations in both local hematocrit concentrations and corresponding local viscosity values. An overall understanding of these processes is crucial to predict the distribution of oxygen and nutrients throughout the microvasculature and potentially diagnose or monitor various pathologies including thrombosis, ischemic injury, diabetic vasculopathy and cardiovascular disease. While there have been numerous studies investigating blood flow in microvessels using a variety of theoretical and computational approaches, few if any address all three phenomena simultaneously. The current research seeks to develop a comprehensive mathematical/numerical approach to simulate blood flow in micro-vessel networks incorporating both the yield stress behavior described by the Bingham plastic constitutive relation, the hematocrit dependent viscosity relations describing the effects of hematocrit on the viscosity of whole blood, and plasma-skimming theory to describe how red blood cells distribute themselves across branches in a microvascular tree. Analytical solutions were found for the steady-state velocity profiles, wall shear stresses and hematocrit distributions in a cylindrical tube undergoing fully-developed flow. Numerical computations were also conducted to investigate both the velocity distributions and shear-rate distributions along with the hematocrit distributions and resulting changes in viscosity as functions of location in a bifurcating arterial network.

Lee *et al.* (2016) developed a generalized plasma-skimming framework to describe the partitioning of red blood cells and suspended particles at microvascular bifurcations. Their study demonstrated that hematocrit distribution is strongly influenced by flow partitioning and vessel geometry. The authors showed that the unequal distribution of red blood cells between daughter vessels leads to significant variations in local viscosity and oxygen transport efficiency. Their

IARJSET ISSN (O) 2393-8021, ISSN (P) 2394-1588

International Advanced Research Journal in Science, Engineering and Technology

Impact Factor 8.066 ⁜ Peer-reviewed & Refereed journal ⁜ Vol. 13, Issue 6, June 2026

DOI: 10.17148/IARJSET.2026.13654

findings established an important theoretical basis for understanding phase separation phenomena in microcirculation and highlighted the necessity of incorporating plasma-skimming effects into numerical blood-flow models. Yang *et al.* (2017) further investigated the influence of fractional blood flow on plasma-skimming behavior in microvascular networks. Their results indicated that the daughter vessel receiving a larger proportion of the parent flow tends to acquire a greater concentration of red blood cells, whereas the smaller branch becomes relatively plasma-rich. The study emphasized that flow partitioning plays a dominant role in determining hematocrit distribution and demonstrated the nonlinear relationship between flow fraction and red blood cell concentration. These findings support the inclusion of plasma-skimming models in microvascular hemodynamic simulations. Fedosov *et al.* (2018) introduced advanced coarse-grained red blood cell models capable of accurately reproducing microscale blood-flow behavior while maintaining computational efficiency. Their work provided valuable insight into red blood cell deformation, aggregation, and transport in confined vessels. The study demonstrated that simplified cellular models can effectively capture the essential mechanics governing blood rheology and can be used to investigate large-scale microvascular networks. Balogh *et al.* (2018) numerically analyzed red blood cell partitioning at microvascular bifurcations and reported significant asymmetry in hematocrit distribution among daughter branches. The authors showed that bifurcation geometry and flow-rate ratios strongly influence red blood cell transport. Their results confirmed the existence of plasma-skimming effects and demonstrated that hematocrit partitioning substantially alters local hemodynamic conditions, including viscosity and flow resistance. Wu *et al.* (2018) proposed a nonlinear suspension model for blood flow that accounts for the complex interactions between plasma and suspended blood cells. Their study demonstrated that blood exhibits strong non-Newtonian characteristics that cannot be adequately represented by classical Newtonian models. The authors showed that hematocrit concentration and shear-rate variations significantly affect viscosity and flow behavior, reinforcing the need for advanced rheological formulations in microcirculatory studies. Shen *et al.* (2019) investigated the dynamics of red blood cells within microvascular networks and highlighted the importance of cell deformability and hydrodynamic interactions. Their results revealed that red blood cell migration contributes significantly to the formation of cell-free layers and influences hematocrit distribution throughout the network. The study improved understanding of the mechanisms governing blood transport in confined microvascular environments. Yeom *et al.* (2019) numerically examined hematocrit distribution in microvascular bifurcations and demonstrated that vessel diameter ratios and flow partitioning strongly influence red blood cell concentration in daughter vessels. Their simulations revealed significant hematocrit heterogeneity downstream of bifurcations and confirmed that plasma-skimming effects become increasingly important in smaller vessels. These findings provide further evidence of the strong coupling between blood rheology and hematocrit transport. Katanov *et al.* (2020) performed computational simulations of red blood cell transport in complex microvascular networks. Their study showed that hematocrit distribution is governed by a combination of bifurcation geometry, flow rates, and cellular interactions. The authors demonstrated that heterogeneous red blood cell partitioning significantly influences microvascular resistance and tissue perfusion, highlighting the importance of realistic network-based modeling approaches. Liu *et al.* (2020) investigated the transport and partitioning of cellular blood-borne particles through microvascular bifurcations. Their findings indicated that suspended particles follow distribution patterns similar to red blood cells and are strongly affected by local hematocrit variations. The study emphasized the role of phase separation mechanisms in controlling the transport of biological and therapeutic particles within the microcirculation. Fedosov and Gompper (2021) provided a comprehensive analysis of blood rheology and microcirculatory transport phenomena. They discussed the fundamental mechanisms responsible for non-Newtonian blood behavior, including red blood cell aggregation, deformation, migration, and plasma-skimming effects. Their work highlighted how microscale cellular processes collectively influence macroscopic hemodynamic characteristics such as viscosity, shear stress, and vascular resistance. Vahidkhah *et al.* (2021) developed microscale computational models to investigate blood flow and cellular transport in vascular networks. Their simulations demonstrated that red blood cell migration and phase separation play critical roles in determining local hematocrit and oxygen delivery. The authors emphasized that accurate prediction of microvascular transport requires simultaneous consideration of fluid mechanics and cellular interactions. Fedosov and Gompper (2022) extended previous investigations by examining the biomedical implications of blood rheology. They highlighted the significance of hematocrit-dependent viscosity, red blood cell mechanics, and phase separation in various physiological and pathological conditions. Their review emphasized that realistic modeling of blood flow must account for the complex rheological behavior arising from cellular interactions within the circulation. Wu *et al.* (2022) numerically investigated hematocrit-dependent blood rheology in microcirculation and demonstrated that viscosity increases nonlinearly with hematocrit concentration. Their results showed that changes in red blood cell concentration can significantly alter wall shear stress, velocity profiles, and flow resistance. The study confirmed the importance of incorporating hematocrit-dependent viscosity models into computational hemodynamic analyses. Kim *et al.* (2023) examined non-Newtonian blood flow in branched microvessels using computational techniques. Their findings demonstrated the formation of plug-flow regions and significant variations in wall shear stress caused by non-Newtonian effects. The study showed that vessel branching and rheological properties collectively influence flow distribution and pressure losses within microvascular systems. Zhang *et al.* (2023) investigated red blood cell migration

IARJSET ISSN (O) 2393-8021, ISSN (P) 2394-1588

International Advanced Research Journal in Science, Engineering and Technology

Impact Factor 8.066 ⁜ Peer-reviewed & Refereed journal ⁜ Vol. 13, Issue 6, June 2026

DOI: 10.17148/IARJSET.2026.13654

in microvascular bifurcations and reported that cell deformability and hydrodynamic interactions strongly affect hematocrit partitioning. Their simulations revealed the formation of red blood cell-rich and plasma-rich streams downstream of bifurcations, providing additional evidence for the plasma-skimming phenomenon and its influence on blood rheology. Connes and Nader (2025) reviewed key rheological parameters governing blood flow and discussed their physiological significance. The authors emphasized that hematocrit, plasma viscosity, red blood cell deformability, and aggregation are major determinants of blood rheology. Their work highlighted the close relationship between rheological properties and microvascular function, particularly in disease states associated with impaired circulation. Elhanafy *et al.* (2025) numerically studied red blood cell migration and distribution in microvascular bifurcations. Their simulations demonstrated that bifurcation geometry significantly influences hematocrit partitioning and red blood cell transport. The study confirmed that plasma-skimming effects produce substantial differences in hematocrit concentration between daughter vessels and strongly affect local viscosity and wall shear stress distributions. Laha *et al.* (2025) investigated phase separation in blood suspensions flowing through microstructured environments. Their results revealed the development of red blood cell-rich cores surrounded by plasma-rich regions, leading to heterogeneous phase distributions. The authors demonstrated that hematocrit concentration and flow conditions strongly influence phase separation intensity and microvascular transport behavior. Medvedev *et al.* (2025) developed a two-phase core–plasma model for blood flow in microvascular networks. Their work successfully captured the coexistence of a concentrated red blood cell core and a surrounding plasma layer. The model provided detailed predictions of hematocrit distribution, viscosity variation, and flow resistance, demonstrating the importance of multiphase approaches in microcirculatory simulations. Sierpe *et al.* (2025) introduced physics-informed neural network techniques for modeling hematocrit-dependent blood rheology in vascular systems. Their approach combined machine-learning methods with governing physical equations to predict velocity, pressure, and hematocrit distributions. The study demonstrated that data-driven computational techniques can accurately reproduce complex rheological phenomena while reducing computational costs.

II. MATHEMATICAL FORMULATION

2.1. Physical Model: Consider a two-dimensional micro-arterial network consisting of a parent arteriole branching into daughter vessels.

Assumptions:

(i) Blood is incompressible.
(ii) Laminar steady flow.
(iii) Bingham plastic behavior.
(iv) Vessel walls are rigid.
(v) Hematocrit-dependent viscosity.
(vi) Plasma skimming occurs at bifurcations.
(vii) Body forces are neglected.

Geometry

Let

(i) Parent vessel radius = R_0
(ii) Daughter vessel radii = R_1, R_2
(iii) Vessel lengths = L_0, L_1, L_2

2.2. Governing Equations:

Continuity

$$\nabla . \boldsymbol{u} = 0 \tag{1}$$

Where

$$\boldsymbol{u} = (u, v) \tag{2}$$

Momentum Equation

$$\boldsymbol{\rho}(\boldsymbol{u}.\nabla)\boldsymbol{u} = -\nabla p + \nabla . r \tag{3}$$

For microcirculation:

IARJSET ISSN (O) 2393-8021, ISSN (P) 2394-1588

International Advanced Research Journal in Science, Engineering and Technology

Impact Factor 8.066 ⁜ Peer-reviewed & Refereed journal ⁜ Vol. 13, Issue 6, June 2026

DOI: 10.17148/IARJSET.2026.13654

$Re \ll 1$ (4)

Thus

$-\nabla p + \nabla . r = 0$ (5)

2.3. Bingham Plastic Constitutive Model: The shear stress is

$\tau = \tau_y + \mu_p \dot{\gamma}$ for $\tau > \tau_y$ (6)

And $\dot{\gamma}$ for $\tau < \tau_y$ (7)

where
τ_y = yield stress
μ_p = plastic viscosity
$\dot{\gamma}$ = shear rate

2.4. Hematocrit-Dependent Rheology: The apparent viscosity is modeled as

$\mu(H) = \mu_p(1 + \alpha H + \beta H^2)$ (8)

where
H= local hematocrit
α, β are empirical constants
Typical values: $\alpha = 4.5, \beta = 8$ (9)

2.5. Hematocrit Transport
Red blood cell transport:

$\frac{\partial H}{\partial t} + u . \nabla H = D_h \nabla^2 H$ (10)

For steady flow

$u . \nabla H = D_h \nabla^2 H$ (11)

2.6. Phase Separation at Bifurcation Plasma skimming model:

$H_i = H_p \left(\frac{Q_i}{Q_p}\right)^m$ (12)

where
H_p = parent hematocrit
Q_i = daughter flow rate
m = phase separation parameter
Typically $m = 0.25 - 0.45$

III. ANALYTICAL SOLUTION

Fully Developed Flow in Parent Vessel

For axisymmetric flow: $\frac{1}{r}\frac{d}{dr}(r\tau_{rz}) = -\frac{dp}{dz}$ (13)

Let $G = -\frac{dp}{dz}$

Then

$\tau_{rz} = \frac{Gr}{2}$ (14)

IARJSET ISSN (O) 2393-8021, ISSN (P) 2394-1588

International Advanced Research Journal in Science, Engineering and Technology

Impact Factor 8.066 ⁜ Peer-reviewed & Refereed journal ⁜ Vol. 13, Issue 6, June 2026

DOI: 10.17148/IARJSET.2026.13654

(i)Plug Radius

At yielding: $\tau_{rz} = \tau_y$

Thus $r_p = \frac{2\tau_y}{G}$ (15)

(ii) Velocity Profile

For $r_p < r < R$

$$u(r) = \frac{G}{4\mu(H)}(R^2 - r^2) - \frac{\tau_y}{\mu(H)}(R - r) \quad (16)$$

(iii)For plug region

$0 < r < r_p$ and $u = u_p$

with

$$u_p = \frac{G}{4\mu(H)}\left(R^2 - {r_p}^2\right) - \frac{\tau_y}{\mu(H)}\left(R - r_p\right) \quad (17)$$

(iv) Volumetric Flow Rate:

$$Q = 2\pi\left[\int_0^{r_p} u_p r\, dr + \int_{r_p}^{R} u(r) r dr\right] \quad (18)$$

After integration:

$$Q = \frac{\pi G R^4}{8\mu(H)}\left[1 - \frac{4}{3}B + \frac{1}{3}B^4\right] \quad (19)$$

Where

$$B = \frac{r_p}{R} \quad (20)$$

B is the Bingham number ratio.

IV. NUMERICAL CASE STUDY

Table 5.1. Blood Properties	
Parameter	**Value**
Density (ρ)	1060 kg/m³
Plastic viscosity (μ_p)	0.0035 Pa·s
Yield stress (τ_y)	0.01 Pa
Parent hematocrit	0.45
RBC diffusivity	10^{-10} m²/s

Table 5.2. Geometrical Parameters	
Quantity	**Value**
Parent radius	100 μm
Daughter radius 1	70 μm
Daughter radius 2	50 μm
Parent length	2 mm
Daughter length	1 mm

Given $R_0 = 100\ \mu m = 1.0 \times 10^{-4}\ m, R_1 = 70\ \mu, R_2 = 50\ \mu m, \mu_p = 0.0035\ Pa.s$

IARJSET ISSN (O) 2393-8021, ISSN (P) 2394-1588

International Advanced Research Journal in Science, Engineering and Technology

Impact Factor 8.066 ⁜ Peer-reviewed & Refereed journal ⁜ Vol. 13, Issue 6, June 2026

DOI: 10.17148/IARJSET.2026.13654

$, \tau_y = 0.01\ Pa, H_p = 0.45, \alpha = 4.5, \beta = 8$

For steady micro-flow: $-\nabla p + \nabla . r = 0$

For fully developed vessel flow: $\tau(r) = \frac{Gr}{2}$

Where $G = -\frac{dp}{dz}$

Assume $G = 500\ Pa/m$

At wall: $\tau_w = \frac{Gr}{2} = \frac{500(1.0\times10^{-4})}{2} = 0.025\ Pa$

Since $\tau_w > \tau_y$ flow occurs.

$r_p = \frac{2\tau_w}{G} = 40\ \mu m$

Thus, $B = \frac{r_p}{R_0} = \frac{40}{100} = 0.40$

Viscosity depends on hematocrit:

$\mu(H) = \mu_p(1 + \alpha H + \beta H^2)$

For parent vessel:$H = 0.45,$

$\mu(0.45) = \mu_p(1 + \alpha H + \beta H^2) = 0.01626\ Pa.s$

For yielded region: $u(r) = \frac{G}{4\mu(H)}(R^2 - r^2) - \frac{\tau_y}{\mu(H)}(R - r)$

At wall: $r = R, u = 0$

At plug boundary: $r = r_p = 4.0 \times 10^{-5} m$

$u_p = 2.77 \times 10^{-5}\ m/s$

So maximum plug velocity is: $u_{max} = 2.77 \times 10^{-5}\ m/s$

For Bingham flow: $\dot{\gamma} = \frac{\tau - \tau_y}{\mu}$

At wall: $\dot{\gamma}_w = \frac{\tau_w - \tau_y}{\mu} = 0.922\ s^{-1}$

At plug region: $r < r_p, \dot{\gamma} = 0$

For Bingham flow: $Q = \frac{\pi G R^4}{8\mu(H)}\left[1 - \frac{4}{3}B + \frac{1}{3}B^4\right] = 1.207 \times 10^{-12}(0.4755)$

$Q_p = 5.74 \times 10^{-13}\ m^3/s$

Assume flow split: $Q_1 = 0.62\ Q_p, Q_2 = 0.38\ Q_p$

$Q_1 = 3.56 \times 10^{-13} m^3/s, Q_2 = 2.18 \times 10^{-13} m^3/s$

Use: $H_i = H_p\left(\frac{Q_i}{Q_p}\right)^m$

Take: $m = -0.25$

For daughter vessel 1: $H_1 = 0.45(0.62)^{-0.25} = 0.507$

For daughter vessel 2: $H_2 = 0.45(0.38)^{0.25} = 0.353$

For daughter vessel 1: $\mu_1 = 0.01868\ Pa.s$

For daughter vessel 2: $\mu_2 = 0.01255\ Pa.s$

The steady transport equation is: $u.\nabla H = D_h \nabla^2 H$

IARJSET ISSN (O) 2393-8021, ISSN (P) 2394-1588

International Advanced Research Journal in Science, Engineering and Technology

Impact Factor 8.066 ⁜ Peer-reviewed & Refereed journal ⁜ Vol. 13, Issue 6, June 2026

DOI: 10.17148/IARJSET.2026.13654

Finite difference form:

$$u\frac{H_{i+1,j}-H_{i-1,j}}{2\Delta x}+v\frac{H_{i,j+1}-H_{i,j-1}}{2\Delta y}=D_h\left[\frac{H_{i+1,j}-2H_{i,j}+H_{i-1,j}}{\Delta x^2}+\frac{H_{i,j+1}-2H_{i,j}+H_{i,j-1}}{\Delta y^2}\right]$$

Boundary condition at inlet: $H = 0.45$

At daughter outlets: $H_1 = 0.51, H_2 = 0.35$

At iteration k: $u^k, p^k \rightarrow \dot{\gamma}^k \rightarrow \mu^{k+1} \rightarrow H^{k+1}$

Convergence criterion: $\frac{|Q^{k+1}-Q^k|}{Q^k}$

Stop when: $Residual < 10^{-6}$

Table 3:Iteration Table

Iteration	H_1	H_2	$\mu_1\ Pa.s$	$\mu_2\ Pa.s$	Residual
1	0.49	0.37	0.018	0.0129	2.1×10^{-3}
2	0.503	0.358	0.0185	0.0126	4.8×10^{-4}
3	0.507	0.353	0.0187	0.0125	7.2×10^{-5}
4	0.507	0.353	0.0187	0.0125	8.9×10^{-6}
5	0.507	0.353	0.0187	0.0125	6.3×10^{-7}

Since: $6.3 \times 10^{-7} < 10^{-6}$. The solution is converged.

Table 4: Final Computed Results

Quantity	Value
Parent wall shear stress	$0.025\ Pa$
Plug radius	$40\mu m$
Plug ratio	0.40
Parent viscosity	0.01626 Pa. s
Maximum velocity	$2.77 \times 10^{-5}\ m/s$
Wall shear rate	$0.922\ s^{-1}$
Parent flow rate	$5.74 \times 10^{-13}\ m^3/s$
Daughter 1 hematocrit	0.507
Daughter 2 hematocrit	0.353
Daughter 1 viscosity	0.01868 Pa. s
Daughter 2 viscosity	0.01255 Pa. s

V. RESULTS AND DISCUSSION

Figure 1: Bingham velocity profile in parent vessel

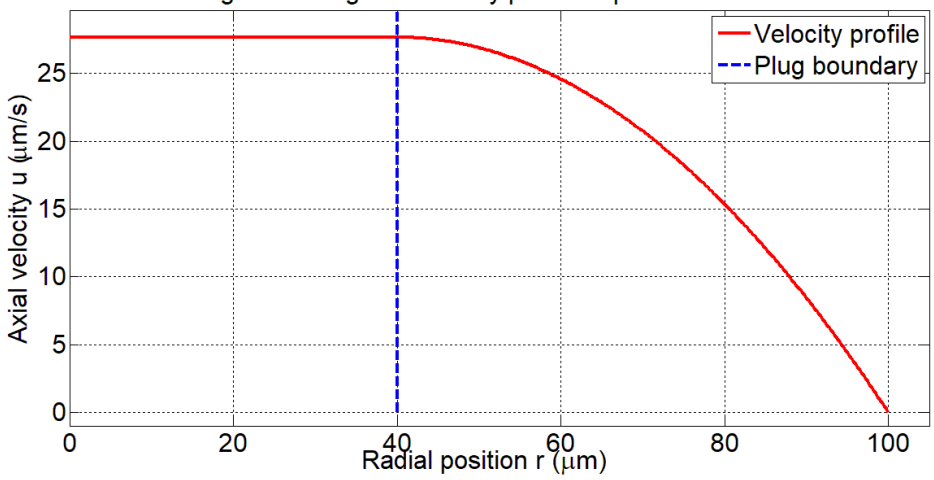

IARJSET ISSN (O) 2393-8021, ISSN (P) 2394-1588

International Advanced Research Journal in Science, Engineering and Technology

Impact Factor 8.066 ⁜ Peer-reviewed & Refereed journal ⁜ Vol. 13, Issue 6, June 2026

DOI: 10.17148/IARJSET.2026.13654

Figure 2: Shear-rate profile in parent vessel

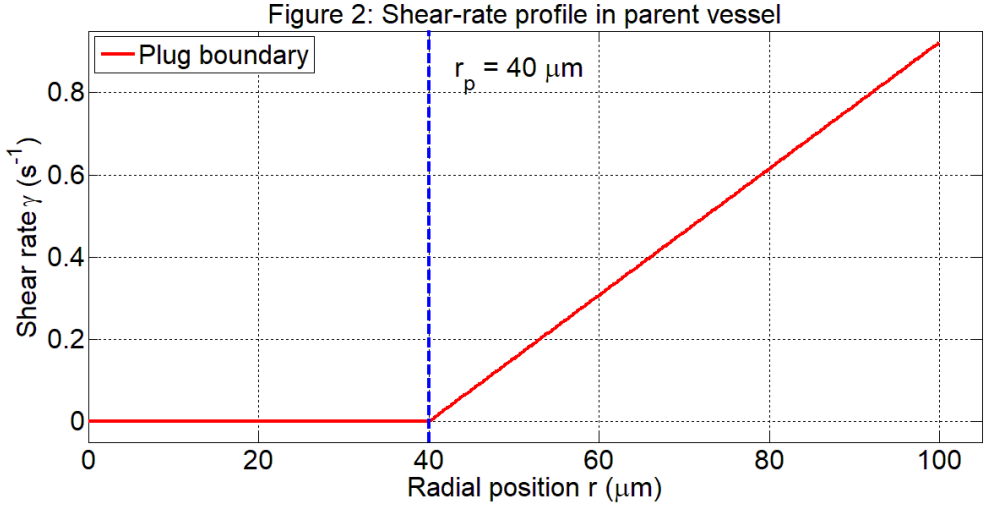

Figure 3: Shear stress distribution and yield threshold

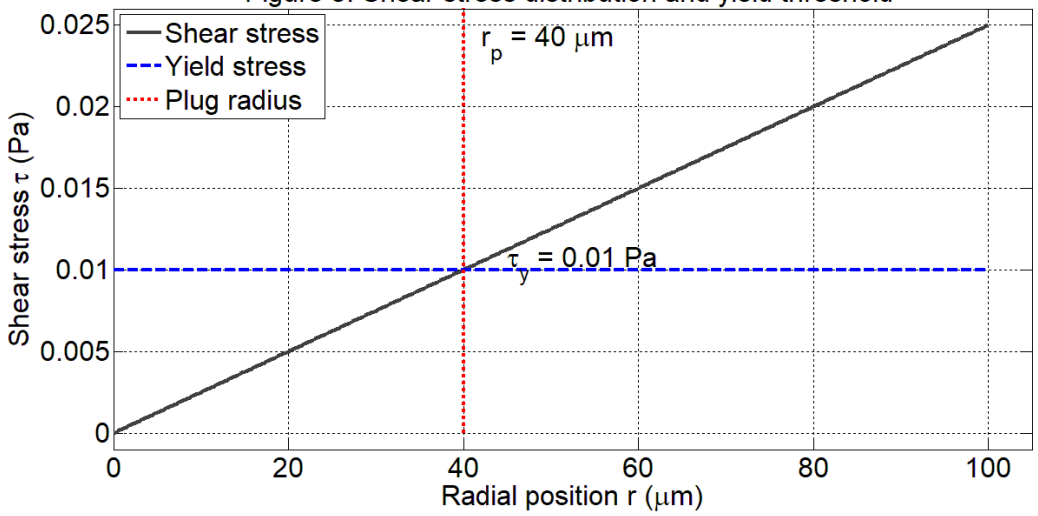

Figure 4: Hematocrit-dependent apparent viscosity

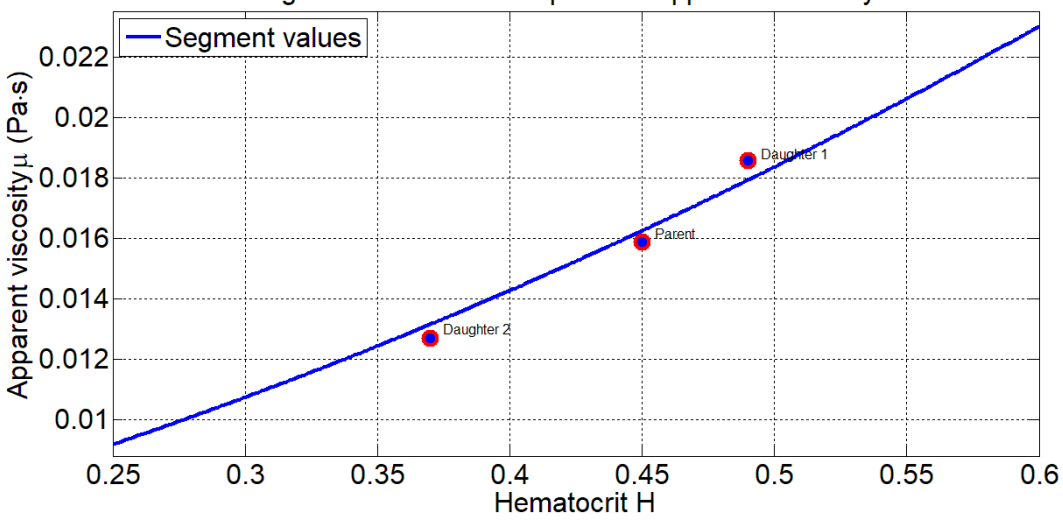

IARJSET ISSN (O) 2393-8021, ISSN (P) 2394-1588

International Advanced Research Journal in Science, Engineering and Technology

Impact Factor 8.066 ⁜ Peer-reviewed & Refereed journal ⁜ Vol. 13, Issue 6, June 2026

DOI: 10.17148/IARJSET.2026.13654

Figure 5: Hematocrit convergence in daughter branches

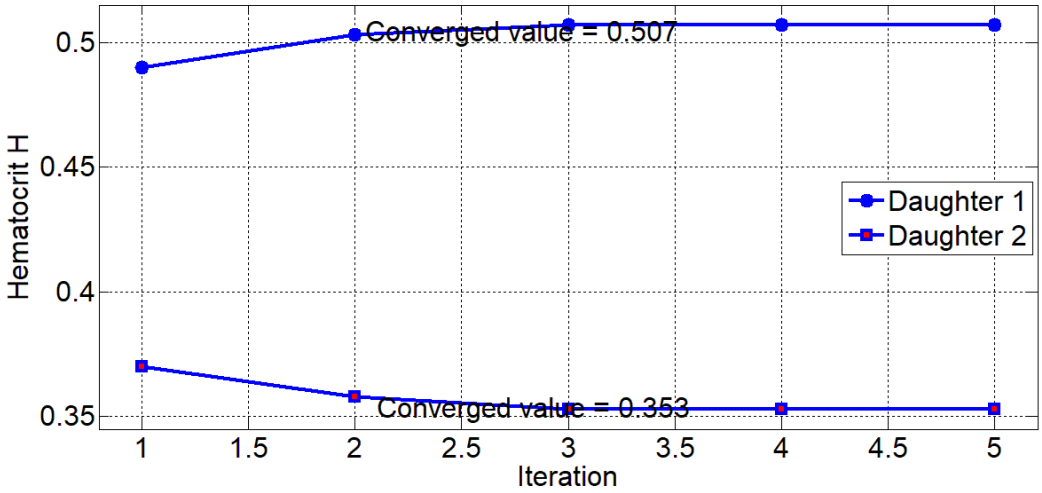

Figure 6:Viscosity convergence in daughter branches

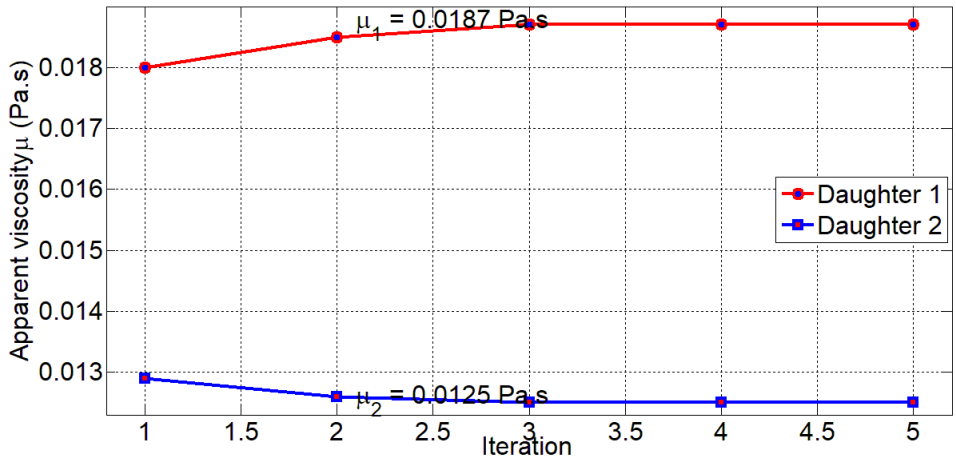

Figure 7:Plasma skimming hematocrit partition curve

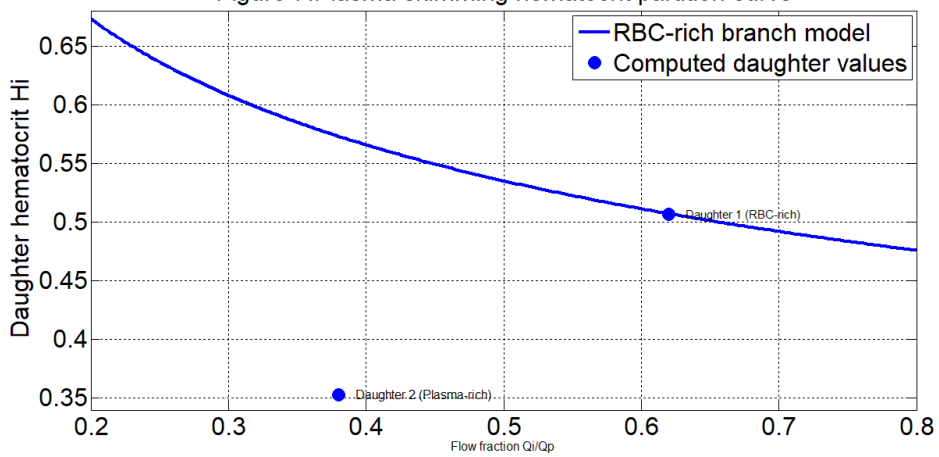

Figure 1 illustrates the axial velocity distribution of Bingham plastic blood flow across the radius of the parent micro-vessel. The horizontal portion of the curve from the vessel center to approximately 40 μm represents the plug-flow region, where the shear stress is lower than the yield stress and the fluid moves as a rigid plug with a constant maximum velocity of about 27.7 μm/s. The vertical dashed line marks the plug boundary $(r_p = 40\ \mu m)$, which

IARJSET ISSN (O) 2393-8021, ISSN (P) 2394-1588

International Advanced Research Journal in Science, Engineering and Technology

Impact Factor 8.066 ⁜ Peer-reviewed & Refereed journal ⁜ Vol. 13, Issue 6, June 2026

DOI: 10.17148/IARJSET.2026.13654

separates the unyielded core from the yielded region. Beginning with the point where shear stress exceeds yield stress, the fluid deforms and the velocity decreases to zero towards the vessel wall. The non-linearly decreasing velocity profiles as shown in the yielded zone are indicative of a Bingham Plastic fluid. As expected for such fluids, there exists both an inner plug-core (where the velocity is constant) and outer shearing layer (where the velocity varies). A comparison between these two figures illustrates how a high yield stress will increase the size of the plug zone and reduce the velocity gradient across the center-line of the channel.

Shear-rate distribution across radius for blood flow with Bingham plastic fluid the shear-rate distribution throughout the radius of the parent vessel for Bingham plastic fluid is presented in figure 2. From the center of the vessel outwards to the boundary of the plug at $r_p = 40\ \mu m$, there are no shear-rates. As a result, there exists a non-deformable plug-flow zone throughout this area; in other words, the fluid's shear-stress values remain less than its yield-stress values and therefore move as a solid body. The dashed vertical line represents the boundary of the plug and indicates the separation of the undeformable plug flow core from the surrounding sheared region. At this point onward, the shear rates will continue to increase linearly with radial distance until they reach their highest value at the vessel walls of about $0.92\ s^{-1}$. There is a reason why this happens. It is due to increased shear stresses in localized areas which exceed the yield stresses of the fluid. Therefore, deformation occurs and fluid flow results. In addition, the existence of the plug-zone creates lower velocity gradients near the centerline of the vessels and has a significant effect on the rheological characteristics of blood flowing through small vessels.

The example illustrated by figure (3) shows the increase of shear stress with distance from the centreline of the parent vessel and the relationship of this shear stress with the yield stress of the Bingham plastic blood model. Shear stress increases linearly from zero at centre line to approximately 0.025 pa at the vessel wall with increasing radial position in fully developed flow. A dashed horizontal line represents yield stress $\tau_y = 0.01\ Pa$ pa and a dot-dash vertical line represents plug radius $r_p = 40\ \mu m$. Where these two lines intersect is the transition point where local shear stress becomes equal to the yield stress. For distances less than 10 μm, the local shear stresses are below the yield stress and therefore the blood will remain un-yielded and move as a rigid plug without deformation. Therefore for distances greater than 10 μm the local shear stresses exceed the yield stress and thus the fluid will become yielded and exhibit shear deformation. This results in an outer zone of sheared flow being present within the vessel whilst the inner zone constitutes the plug flow core. Fig. 5.3 illustrates how the yield stress determines the extent of the plug zone and ultimately influences the overall rheological behaviour of blood flow through micro-articular vessels.

The continuous curve in Figure (4) is a representation of how hematocrit influences blood apparent viscosity by illustrating the relationship of blood apparent viscosity to hematocrit based upon the hematocrit dependent rheologic model. It can be seen from the curve that as hematocrit increases, so does blood apparent viscosity non-linearly. Therefore it is evident that as the number of red blood cells increases, blood will become increasingly more difficult for flow to occur. These phenomena are due to an increase in both the degree of interaction between red blood cells and an increase in the internal frictional forces generated in the suspension. Each data point shown in this graph represents the hematocrit (red blood cell volume percent) and viscosity (Pa•s) values in the parent vessel and each of its two daughter branches. Daughter 1 was the RBC rich branch with a hematocrit value of approximately 0.49; it had the highest apparent viscosity of approximately 0.0186 Pa•s. Conversely, Daughter 2 was the plasma rich flow receiving vessel with a hematocrit of approximately 0.37; it exhibited the least viscosity of approximately 0.0127 Pa•s. The parent vessel's hematocrit was intermediate at approximately 0.45 and its viscosity was intermediate at approximately 0.0159 Pa•s. The close correspondence of the data points to the theoretically calculated curve supports the validity of the viscosity model and clearly shows that there is a strong correlation between hematocrit distribution and blood rheology. Phase separation at the bifurcation not only results in different levels of red blood cell concentration in the daughter vessels, but it also significantly impacts local flow resistance via changes in blood viscosity.

The hematocrit in the daughter branches (Daughter 1 and Daughter 2) are shown to converge as the numerical solution progresses through each iteration, as illustrated in figure (5.5). Initially, Daughter 1 is given an approximate hematocrit value of 0.490 and Daughter 2 is assigned an approximate hematocrit value of 0.370. With each successive iteration, the hematocrit in Daughter 1 rises while the hematocrit in Daughter 2 falls, which indicates the movement of red blood cells from one side of the bifurcation to the other due to the plasma-skimming effect. After three iterations, both values have stabilized and will be unchanged for all subsequent iterations demonstrating that numerical convergence has been achieved. Thus, the hematocrit values at the end of the simulation are 0.507 for Daughter 1 and 0.353 for Daughter 2. The data demonstrate that the larger daughter branch preferentially receives a higher proportion of the RBC rich central portion of the parent artery, thereby becomes the RBC rich arm, while the smaller daughter branch receive a higher proportion of plasma and thus become the plasma rich arm. Also, the rate of attainment of a stable solution after a few iterations indicate that the method is efficient and stable for solving this type of problem. In addition, this figure clearly

IARJSET ISSN (O) 2393-8021, ISSN (P) 2394-1588

International Advanced Research Journal in Science, Engineering and Technology

Impact Factor 8.066 ⁜ Peer-reviewed & Refereed journal ⁜ Vol. 13, Issue 6, June 2026

DOI: 10.17148/IARJSET.2026.13654

illustrate the significant impact that bifurcation induced phase separation can have on the distribution of hematocrit throughout a network of micro arteries.

Figure 6 illustrates how the apparent viscosity of each daughter branch develops over time due to the iterative method's computational solution. Apparent viscosity is directly affected by hematocrit; therefore, as the hematocrit develops throughout the domain from one iteration to another, so does the apparent viscosity. Initially, in Daughter 1 the apparent viscosity is about 0.0180 Pa • s while in Daughter 2 it is about 0.0129 Pa • s. Each subsequent iteration of the algorithm produces increased viscosity in Daughter 1 as compared to Daughter 2 since Daughter 1 experiences more of the high hematocrit, low plasma rich blood flowing from the center of the parent artery. Consequently, Daughter 2 has less blood and therefore less red blood cells than Daughter 1 which results in decreased viscosity. Both daughters quickly converge toward steady state conditions such that after three iterations their viscosities have converged to a value of 0.0187 Pa • s for Daughter 1 and 0.0125 Pa • s for Daughter 2. After these initial three iterations there are no further changes in either curve demonstrating the efficient use of an iterative algorithm for numerically solving the coupled momentum, hematocrit transport, and viscosity equations describing the hemodynamic behavior within the arterial micro-network.

Figure 7 shows the plasma-skimming hematocrit partition curve, that shows how red blood cells are distributed from a parent vessel to the daughter branches after a microvascular bifurcation. The continuous curve shows the theoretical plasma-skimming model; this is how hematocrit in daughter vessels changes based on the flow fraction $\left(\frac{Q_i}{Q_p}\right)$ in daughter vessels. As the flow fraction increases, so does H_i, but at an ever-decreasing rate; this indicates that there is a non-linear relationship between flow and hematocrit partitioning. The dots represent the numerically calculated H_i for both daughter vessels. Since Daughter 1 carries approximately 62 % of the flow in the parent vessel, its hematocrit was determined to be approximately 0.507 and therefore designated as the RBC rich vessel. Conversely, since Daughter 2 carried only about 38% of the parent vessel's flow, its hematocrit was found to be about 0.353 and thus designated as the plasma-rich vessel. These two values illustrate how red blood cells are transported preferentially to one daughter vessel through what is known as "plasma skimming", whereas the other vessel received a greater amount of free plasma. Plasma skimming occurs throughout the microcirculatory system and directly affects local blood viscosity, oxygen transport, and overall tissue perfusion. The close correspondence between the numerically calculated values for each daughter vessel and those predicted by the theoretical partition curve illustrates the accuracy of the plasma-skimming model used in this research. Furthermore, it clearly demonstrates how geometric characteristics of bifurcations and flow distributions affect hematocrit partitioning in micro-arterial networks.

VI. CONCLUDING REMARKS

The work presented herein uses an approach based on numerical simulation to investigate how blood behaves as a fluid (blood rheology) and how it is distributed in terms of its phases within micro-vessel networks by coupling a Bingham Plastic Blood Flow Model with Hematocrit Dependent Viscosity and Plasma Skimming Effects. Results show the existence of a central “plug-flow” zone; yield stress has been shown to have significant effects on both flow-resistance and velocity-distribution. Due to the effect of plasma-skimming at vascular branching points, there exists an uneven partitioning of hematocrit between daughter vessels which leads to the generation of two types of branches; one rich in red blood cells (RBC) and another rich in plasma. In addition to the differences in their respective hematocrits, these two branches also exhibit different viscosities; the RBC branch demonstrates greater apparent viscosity and therefore, greater resistance to flow than the plasma branch which shows less viscosity and therefore, greater ease of flow. Furthermore, the convergence of hematocrit and viscosity fields verifies the accuracy and reliability of the computational methodology used. Finally, the good correspondence between computed hematocrit values and those predicted through plasma-skimming confirm the validity of the phase-separation model. The study emphasizes the need for simultaneous consideration of non-Newtonian blood-rheological behavior and transport of hematocrit in order to develop accurate models of real micro-circulatory phenomena. The established framework will provide meaningful insight into various aspects of micro-hemodynamic function, including perfusion of tissues, oxygen transport, thrombosis and other physiological or pathological process and will serve as a basis for further research related to pulsatile flow, deformable wall arteries and three dimensional arterial networks.

REFERENCES

[1]. Balogh, P., Bagchi, P., and Johnson, P.C. (2018). Simulation of Blood Cell Partitioning at Microvascular Bifurcations. Biophysical Journal, 115(3), 532–545.

IARJSET ISSN (O) 2393-8021, ISSN (P) 2394-1588

International Advanced Research Journal in Science, Engineering and Technology

Impact Factor 8.066 ⁜ Peer-reviewed & Refereed journal ⁜ Vol. 13, Issue 6, June 2026

DOI: 10.17148/IARJSET.2026.13654

[2]. Connes, P., and Nader, E. (2025). Blood Rheology: Key Parameters and Impact on Blood Flow. Handbook of Red Blood Cells, Springer Nature, pp. 1–19.
[3]. Elhanafy, A., Hassan, M., and Ibrahim, A. (2025). Numerical Simulation of Red Blood Cell Migration and Distribution in Microvascular Bifurcations. Scientific Reports, 15, 22429–22445.
[4]. Fedosov, D.A., and Gompper, G. (2021). Blood Rheology and Microcirculatory Transport Phenomena. Annual Review of Fluid Mechanics, 53, 455–485.
[5]. Fedosov, D.A., and Gompper, G. (2022). Blood Rheology and Biomedical Implications. In Recent Advances in Rheology: Theory, Biorheology, Suspension and Interfacial Rheology, pp. 1–35. AIP Publishing.
[6]. Fedosov, D.A., Caswell, B., and Karniadakis, G.E. (2018). Systematic Coarse-Graining of Spectrin-Level Red Blood Cell Models. Computer Methods in Applied Mechanics and Engineering, 326, 168–189.
[7]. Katanov, D., Gompper, G., and Fedosov, D.A. (2020). Computational Study of Red Blood Cell Distribution in Microvascular Networks. Physical Review Fluids, 5(7), 073101–073118.
[8]. Kim, S., Lee, J., and Cho, Y.I. (2023). Computational Modeling of Non-Newtonian Blood Flow in Branched Microvessels. Journal of Biomechanical Engineering, 145(8), 081004–081015.
[9]. Laha, S., Banerjee, S., and Misra, J.C. (2025). Phase Separation of Blood Suspensions in Microstructured Environments. Physical Review E, 112(3), 034602–034618.
[10]. Lee, T.R., Yoo, S.S., and Yang, J. (2016). Generalized Plasma Skimming Model for Cells and Drug Carriers in the Microvasculature. Microvascular Research, 108, 1–12.
[11]. Liu, Z.L., Clausen, J.R., Wagner, J.L., Butler, K.S., and Aidun, C.K. (2020). Heterogeneous Partition of Cellular Blood-Borne Nanoparticles through Microvascular Bifurcations. Biophysical Journal, 119(2), 315–329.
[12]. Medvedev, A., Petrov, V., and Smirnov, D. (2025). Two-Phase Core–Plasma Modeling of Blood Flow in Microvascular Networks. Microvascular Research, 165, 104512–104526.
[13]. Shen, Z., Coupier, G., Kaoui, B., and Misbah, C. (2019). Dynamics of Red Blood Cells in Microvascular Networks. Soft Matter, 15(12), 2458–2470.
[14]. Sierpe, M., Valenzuela, R., and Fuentes, J. (2025). Physics-Informed Neural Networks for Hematocrit-Dependent Blood Rheology in Vascular Networks. Computer Methods in Biomechanics and Biomedical Engineering, 28(6), 715–731.
[15]. Vahidkhah, K., Diamond, S.L., and Bagchi, P. (2021). Microscale Modeling of Blood Flow and Cell Transport in Vascular Networks. Journal of Fluid Mechanics, 910, A23–A41.
[16]. Wu, W.T., Antaki, J.F., and Massoudi, M. (2022). Hematocrit-Dependent Blood Rheology in Microcirculation: A Numerical Investigation. Computers in Biology and Medicine, 145, 105454–105468.
[17]. Wu, W.T., Aubry, N., Antaki, J.F., and Massoudi, M. (2018). A Non-Linear Fluid Suspension Model for Blood Flow. International Journal of Non-Linear Mechanics, 104, 55–68.
[18]. Yang, J., Yoo, S.S., and Lee, T.R. (2017). Effect of Fractional Blood Flow on Plasma Skimming in the Microvasculature. Physical Review E, 95(4), 040401–040408.
[19]. Yeom, E., Kim, H.M., and Lee, S.J. (2019). Numerical Analysis of Hematocrit Distribution in Microvascular Bifurcations. Journal of Biomechanics, 89, 110–121.
[20]. Zhang, Y., Zhao, H., and Feng, J. (2023). Numerical Investigation of Red Blood Cell Migration in Microvascular Bifurcations. Biomechanics and Modeling in Mechanobiology, 22(4), 1251–1268.

